Global NEST Journal, Vol 27, No 7, 07439

Green energy management in electric vehicles with regenerative braking using super capacitors and batteries

Kannan Kandavelu[1]*, Mahalakshmi Gunasekaran[2], Anbuchezian Ashokan[3] and Silambarasan Rajendran[4,5]

[1]Department of Electrical and Electronics Engineering, Annapoorana Engineering College (Autonomous), Seeragapadi, Salem, 636308, Tamil Nadu, India.

[2]Department of Electrical and Electronics Engineering, Sri Krishna College of Engineering and Technology (Autonomous), Coimbatore, 641008, Tamil Nadu, India.

[3]Department of Civil Engineering, Annapoorana Engineering College (Autonomous), Seeragapadi, Salem, 636308, Tamil Nadu, India.

[4]Department of Mechanical Engineering, Annapoorana Engineering College (Autonomous), Seeragapadi, Salem, 636308, Tamil Nadu, India.

[5]Department of Mechanical Engineering, Saveetha School of Engineering, Saveetha Institute of Medical and Technical Sciences, Chennai, Tamil Nadu, India.

Received: 11/03/2025, Accepted: 02/07/2025, Available online: 09/07/2025

*to whom all correspondence should be addressed: e-mail: k.kannan79@gmail.com

https://doi.org/10.30955/gnj.07439

Graphical abstract

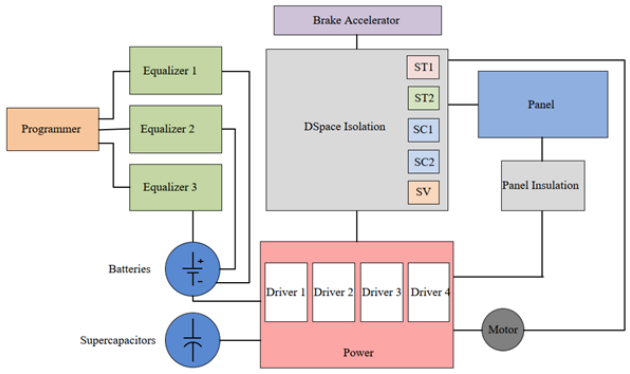

Abstract

This work presents the design and implementation of an energy management system for electric vehicles utilizing regenerative braking. The hybrid power supply comprises a lithium-ion battery bank and a supercapacitor bank. Bidirectional DC-DC converters are employed to manage power flow between the energy storage elements and the DC motor. Regenerative braking allows kinetic energy recovery during deceleration, which is stored in the supercapacitors due to their high power density. The supercapacitors also handle high current demands during acceleration, reducing battery stress. Passive equalization circuits are used for the batteries and supercapacitors to avoid overvoltage conditions. The control system is implemented in MATLAB/Simulink and hardware-in-the-loop testing is performed with a dSPACE platform. Experimental results demonstrated up to 65% regeneration efficiency, with good agreement between simulated and practical values. The supercapacitors successfully supplied momentary high current loads, avoiding premature current limitation by the battery protection system. The results confirm the feasibility of the proposed architecture for electric vehicle applications requiring high power and energy recovery.

Keywords: Regenerative braking, Supercapacitors, Energy management, Electric vehicles, Bidirectional DC-DC converters

1. Introduction

Electric vehicles have gained increasing attention in recent years due to environmental concerns and the need for sustainable transportation solutions. However, some key limitations persist, including relatively short driving range and high battery costs. Research has focused on hybrid energy storage systems and regenerative braking capabilities to address these issues. This work explores an electric vehicle architecture consisting of a lithium-ion battery bank as the main energy source, supplemented by a supercapacitor bank to handle high power demands. Bidirectional DC-DC converters are designed to control power flow between the storage elements and the traction motor.

During deceleration, the motor can operate as a generator to recover some of the vehicle's kinetic energy. This regenerative braking process charges the supercapacitors, using their high-power density and efficient charging capabilities. The supercapacitors also supply momentary high current loads during acceleration events, avoiding over-stressing the batteries. Passive balancing circuits are implemented for the supercapacitors and batteries to prevent overvoltage shutdowns.

The proposed system is modeled in MATLAB/Simulink, allowing rapid design iteration through simulations. The control logic is deployed on a dSPACE real-time platform to enable hardware-in-the-loop testing. Custom circuit

boards were developed for the DC-DC converters, gate drivers, sensors, and auxiliary systems. The experimental test bench uses a permanent magnet DC motor coupled to a flywheel load.

Abdelghany *et al.* (2022): Proposed multi-level model predictive control for wind farm and hydrogen storage system to produce hydrogen fuel for vehicles while meeting electric and contractual loads. Beatrice *et al.* (2024): Studied hybrid storage systems in hybrid electric vehicles to reduce battery cycling degradation under real driving conditions.Charoen-amornkitt *et al.* (2023): Assessed battery swapping systems for electric motorcycles in Thailand, Vietnam, Malaysia and Indonesia for energy and emissions reduction.Chen *et al.* (2021): Surveyed key techniques and perspectives on equivalent consumption minimization strategy for hybrid electric vehicles.Deng *et al.* (2022): Developed deep reinforcement learning based energy management for fuel cell hybrid railway vehicles accounting for fuel cell aging. Deng *et al.* (2021): Proposed adaptive Pontryagin's minimum principle model predictive control strategy for fuel cell hybrid railway vehicles. Eckert *et al.* (2021): Optimized gear shifting and fuzzy logic power-split control in hybrid electric vehicles for emissions and energy reduction without impact on battery life.Falvo *et al.* (2011): Proposed integrated sustainable urban mobility system including metro-transit and electric vehicles with renewable energy charging infrastructure. Frasci *et al.* (2022): Analyzed hybrid electric vehicle with turbulent jet ignition engine experimentally and through simulation for efficiency, emissions and range optimization.Hasan *et al.* (2021): Reviewed lithium-ion battery electric vehicle systems, energy management, challenges and issues.Hu *et al.* (2024): Performed analysis on reinforcement learning based energy management in electric vehicles through algorithm, granularity, hyperparameters and reward function.Icaza-Alvarez *et al.* (2023): Developed long term electrification planning for Cuenca, Ecuador with 100% renewable energy under decentralized configuration. Jannesar Niri *et al.* (2024): Reviewed sustainability challenges throughout electric vehicle battery value chain including raw materials, manufacturing and recycling.Khammassi *et al.* (2024): Assessed electric vehicle adoption and energy transition policy in Tunisia using a sustainable transport index.Li *et al.* (2024): Investigated decision-making for sustainable urban transportation through innovative mobility solutions to reduce emissions.Liguo *et al.* (2023): Empirically evaluated role of hybrid electric vehicle technology innovation in reducing emissions in knowledge based economies.Lu *et al.* (2023): Proposed neural network energy management strategy with optimized input features for plug-in hybrid electric vehicles.Payri *et al.* (2012): Developed stochastic equivalent consumption minimization strategy approach for hybrid electric vehicles without a priori drive cycle.Pecolt *et al.* (2023): Tested electric power system optimization application for hybrid electric vehicle.Qureshi *et al.* (2021): Proposed electric vehicle energy management and charging scheduling system for sustainable cities.Rauf *et al.* (2024): Reviewed artificial intelligence applications in electric vehicles for sustainable environmental impact.Rele *et al.* (2023): Developed hybrid algorithm combining local search and particle swarm optimization for large scale electric vehicle routing. Ritzmann *et al.* (2020): Formulated optimization method for hybrid electric vehicle energy and emissions management with exhaust aftertreatment. Sulaiman *et al.* (2018): Reviewed optimization of energy management systems for fuel cell hybrid electric vehicles. Verma *et al.* (2021): Conducted comprehensive review on energy storage technologies including batteries and ultracapacitors in hybrid electric vehicles. This study aimed to evaluate the real-world fuel consumption of two Honda parallel HEVs compared to a conventional Honda ICEV. Honda's Integrated Motor Assist (IMA) mild hybrid and third generation IMA full hybrid systems were analyzed. On-road testing was conducted in the Lisbon, Portugal area under various driving cycles representing urban, extra-urban, highway, and mixed conditions. Five driver profiles were tested from very slow to very aggressive. Testing was performed using a portable computer datalogger to record real-time vehicle data.

Various operating scenarios are evaluated, including acceleration, constant speed cruising, and regenerative braking. The supercapacitors successfully handle the high current transients during acceleration and charging, while the batteries provide steady discharge currents. Energy transfer efficiencies up to 65% are demonstrated during braking, reasonably matching theoretical predictions. The results help validate the concept of hybrid energy storage and bidirectional power flow for electric vehicle applications.

Future work may involve integrating a grid-connected battery charger to enable full vehicle system implementation. Advanced control algorithms could also improve efficiency and expand operational range. Electric vehicles can become more viable transportation alternatives by overcoming limitations such as short driving distance per charge. The hybrid energy supply and regenerative braking techniques explored in this project represent important steps toward sustainable and efficient electric mobility.

2. Materials and methods

2.1. Circuit design and simulation

The overall system was modeled in MATLAB/Simulink to allow rapid design iterations through simulations. The bidirectional DC-DC converters were designed to interface the battery, supercapacitor, and DC motor. A buck-boost topology was chosen for its ability to step up and down voltage as needed. The converters were controlled using PI controllers to regulate current flow based on reference values. PWM signals were generated to drive the converter switches. Simulations were run to tune the control loop gains and validate expected performance.

The battery bank consisted of 27 lithium-ion cells connected in series, offering a nominal 96V output. Passive balancing circuits were implemented to avoid cell under or overvoltage conditions during operation. The

supercapacitor bank contained 23 modules rated at 58F, 16V, connected in parallel combinations to provide 134V nominal voltage.

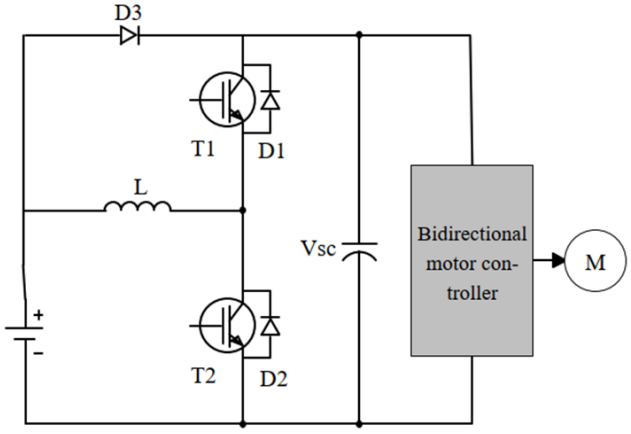

Figure 1. Hybrid Energy Management System.

Differently from the projects presented in **Figure 1**, it maintains the supercapacitor bank connected directly to the DC bus to supply the power peaks required by the electric motor. The battery bank, positioned on the side of lower tension, is connected to the supercapacitor bank through an energy converter and by the diode D3 (34).

This system operates according to the vehicle's power requests. In conditions normal operating conditions, the battery supplies energy to the DC bus and thus the voltage of the supercapacitors can be maintained at high levels and greater than those of the other source (in this case if diode D3 is reverse biased). Suppose the power request is greater than the nominal capacity of the bidirectional DC-DC converter (acceleration process). In that case, the voltage at the bus cannot be maintained, and so the battery supplies power through diode D3 and also by the converter.

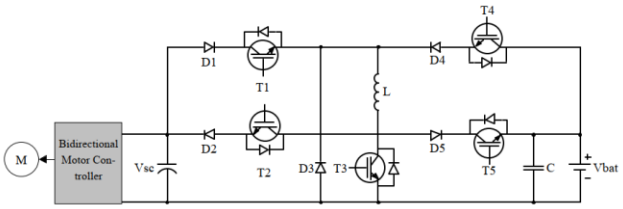

Figure 2. Universal bidirectional DC-DC converter.

During the regeneration process, energy flows directly to thesupercapacitors. Suppose the bus voltage rises above the maximum values permitted. In that case, energy will be sent to the batteries by operation as a step-down of the converter bidirectional. In this way, the battery is charged in a controlled manner. The bidirectional DC-DC converters presented so far are capable of process energy in two directions, but performing only one function (lowering or elevator). Generally, the converter operates as Buck in braking processes regenerative and as a Boost in acceleration processes. However, if the bus voltage is less than that of the battery, the converter operations must be reversed. That way, a universal bidirectional converter capable of operating in both directions must be used andwith lifting and lowering functions (38). The circuit that meets these requirements is represented in **Figure 2**.

An embedded control system was modeled to manage power flow between sources based on SOC and vehicle acceleration/braking conditions. This high-level controller determined the DC-DC converters' reference currents and the converter switches' gate signals. Protection systems were incorporated to disable operation during fault events.

This converter is composed of five transistors (Tl to T 5) with their respective diodes in antiparallel and with two power diodes (DI to DS), during operation only one of the transistors operates through gate pulses (PWM), and the others they remain running or open depending on the purpose performed. Thus, losses due to switching are smaller than those of conventional converters (38). Suppose the supercapacitor voltage is lower than the battery voltage. In that case, the converter must operate as an elevator to bring the energy of regenerative processes to the second source - In this case, transistors Tl and T5 remain in conduction, while T2 and T4 remain turned off; the P WM Signal is applied to T3 (the Boost converter is composed of the elements, T3, T5, L, DI and DS). Maintaining the same condition, the converter must operate as a step-down in the processes acceleration, sending battery energy to the DC bus (where the bank connects of supercapacitors) - The transistors T l, T 3 and T 5 remain off, while T2drives all the time; the P WM Signal is applied to T4 (the Buck converter is composed by elements T2, T4, L, D2, m and D4) (38).

2.2. Hardware implementation

A scaled-down prototype was built with a 90V battery bank, 66V supercapacitor bank, and 24V permanent magnet DC motor coupled to a flywheel load. The bidirectional converters were constructed using MOSFETs with high current capability and fast switching speeds. Gate driver circuits were implemented to amplify the PWM signals from the DSP and provide isolation.

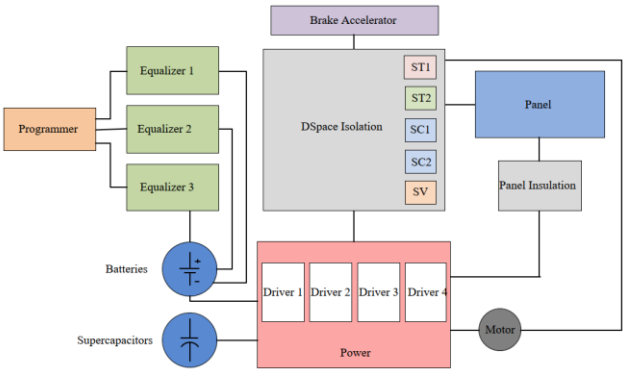

Figure 3. General diagram of the bench prototype.

The "Programmer" board is tasked with programming the dedicated integrated circuits (ICs) for battery equalization, setting critical parameters such as minimum voltage thresholds and operational limits for overload and short-circuit protection during charging and discharging cycles, among other functionalities as shown in **Figure 3**. The "Equalizer", "Equalizer 2", and "Equalizer 3" boards host

the equalization circuits and auxiliary power sources, and also incorporate additional components for battery temperature equalization, including power transistors and resistors. Each board also features connectors designed for the electrical linkage of battery units.

The "DSpace Isolation" board is equipped with auxiliary power sources, digital and analog isolators, and operational amplifiers. Its primary role is to safeguard the DSpace platform and the connected computer system against potential issues or accidents arising from other systems. Furthermore, the setup includes five small modules: "STL" (Voltage Sensor 1), "ST2" (Voltage Sensor 2), "SCl" (Correction Sensor 1), "SC2" (Current Sensor 2), and "SV" (Speed Sensor), which are integral to the preprocessing of signals and corrections.

The "Accelerator and Brake" system comprises two potentiometers; one regulates the armature voltage of the DC motor during operation, while the other modulates the braking current, which is directly proportional to the braking torque.

The "Panel" features displays for monitoring battery voltages and uses LEDs (Light-emitting diodes) to indicate the system's current status. It is also equipped with interfaces for signaling the presence or absence of power at the charging station (PA), activating or supplying gate pulses to the IGBT (Insulated-Gate Bipolar Transistor) drivers, or performing a system reset. The "Insulation Panel" adapts and isolates the voltages from the battery bank and supercapacitors, preparing them for further processing.

Finally, the "Power" board aggregates key components of the bidirectional converter and includes auxiliary power sources, current sensors, and IGBT drivers (Driver 1, Driver 2, Driver 3, and Driver 4), all interconnected via connectors. Each driver is tasked with receiving gate pulses (0 and 5V) and converting them to 15V with galvanic isolation, utilizing an isolated power source that maintains the same potential at its output.

Hall effect sensors measured the inductor currents for feedback control. The DC motor had an integrated tachometer to measure shaft speed. Analog signal conditioning circuits adapted the sensor outputs for the digital controller. Optocouplers provided isolation for fault signals and control inputs like accelerator/brake pedal position. Custom PCBs were fabricated for the converters, gate drivers, and auxiliary systems.

The control logic and regulators were coded in Simulink then compiled to run on a dSPACE DS1006 processor board. The dSPACE provided ADCs, PWM outputs, digital I/O, and interfacing with MATLAB/Simulink for hardware-in-the-loop testing. Protections were included to disable operation during overcurrent or voltage faults. Data was logged in the dSPACE ControlDesk interface.

3. Experimental setup and procedure

The test bench was used to evaluate the performance of the prototype. Acceleration tests verified the supercapacitors could supply the temporary high current loads. Constant speed and cruising scenarios validated steady-state operation. Regenerative braking tests were conducted by increasing the motor load to demonstrate charging of the supercapacitors from recovered energy. The dSPACE controller successfully coordinated the switching states of the converters in response to operating conditions.

Current, voltage, and speed measurements were recorded to quantify the energy flows during the tests. Regeneration efficiency was determined based on the energy recovered versus the maximum possible. Results were analyzed relative to theoretical predictions from simulations. This experimental evaluation demonstrated the feasibility and effectiveness of the hybrid energy storage system with bidirectional converters. The test bench provided a flexible platform for validating the system integration before installing in an actual vehicle.

The project's circuitry and their respective boards provide a comprehensive view of the energy management and conversion processes, augmented by a control system implemented in Simulink and executed on the platform. The DC motor utilized in this setup is equipped with a tachometer attached to its shaft, facilitating the acquisition of angular velocity data for the associated preprocessing module.

At the opposite end, a disk with a mass of 4.27 kg, a radius of 21.3 cm, and a moment of inertia of 0.097 kg·m² simulates the inertia of a small-scale vehicle. This setup poses a question on efficiently capturing the necessary kinetic energy during regenerative braking phases. The entire assembly is currently stationed in the laboratory. After introducing all system components, their complete interconnection is showcased in **Figure 4**. Connections between digital outputs and inputs were established using pairs of headers connected by flat cables, chosen for their flexibility and suitability for transmitting low-power signals.

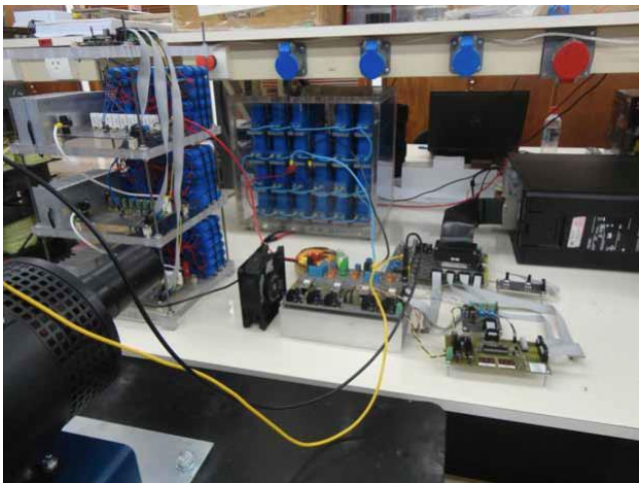

Figure 4. Complete experimental setup visualized.

Energy accumulators are linked to the "Power" board via "banana" type connectors, alongside the inductor (L) and the DC motor. A heatsink, approximately covering its perimeter, is situated between the transistors, with forced ventilation provided by a fan located on the left side of the assembly.

The control system's operational signals are transmitted via soldered cables running from the "DSpace+ Isolation" board to the desktop computer, positioned to the right in **Figure 4**. Finally, the power for all auxiliary sources is supplied by isolated DC-DC converters powered by this computer's supply, thus eliminating the need for additional hardware within the system.

4. Results and discussion

The experimental test bench provided the ability to validate the operation of the hybrid energy storage system and control logic. Various scenarios were evaluated to demonstrate the key functions of the prototype, including acceleration events, constant speed cruising, and regenerative braking. During acceleration from standstill, the supercapacitors supplied the temporary high current demanded by the motor. Currents over 8A were drawn, while the batteries provided under 2A, avoiding stress on the cells. The supercapacitors exhibited minimal voltage sag during these heavy loads due to their low equivalent series resistance. As speed stabilized, the batteries became the main power source.

In this section, we delve into the system's overall behavior as observed through simulations conducted within the Simulink environment. The focus here is on outlining the system's operation, which is based on the interactions between batteries, supercapacitors, and a mechanically applied resistive torque, assumed to be constant for the purposes of this discussion. Beginning with the primary inputs—namely, the accelerator and brake signals—we aim to shed light on the dynamic processes outlined in Chapter 3. Furthermore, aspects related to the regeneration of energy and performance metrics during braking phases, along with the corresponding equations, will be scrutinized to assess their accuracy and predictability.

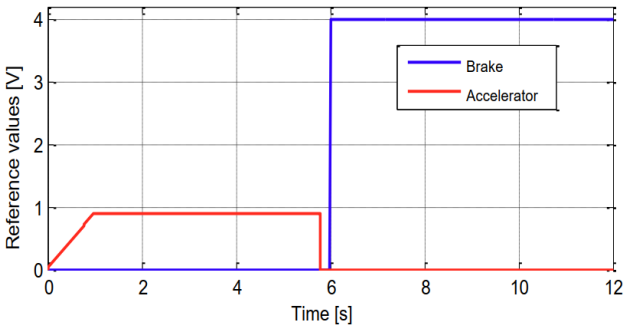

Figure 5. Accelerator and brake signals.

The energy exchange dynamics between the battery accumulators and the current motor are illustrated through colored areas generated in the simulation results, highlighting instances of energy transfer. Within these areas, smaller rectangles identify key elements of the system, where notations such as BSC→M, M→BSC, and BB→BSC represent energy flows from the supercapacitor bank to the motor, from the motor to the supercapacitor bank, and from the battery bank to the supercapacitor bank, respectively.

The initial graphs are derived under V_bsc = 240V, V_eb = 96V, and T_m = 0.50N.m. Interactions with the accelerator and brake are essential to facilitate the intended system functionalities, as these represent the control inputs from the user. **Figure 5** showcases the resultant behavior, providing insight into accelerator and brake signals.

The throttle signal indicates that the average voltage at the DC motor terminals reaches 90% (144V) in the interval of 1s, which is maintained up to 5.8s; From then on, there is no further transfer of energy to the machine. The brake is applied at 6s in the form of a step (sudden braking), forcing the absorption of a current Ia equal to 4A, maintained until the end of the simulation. The variation of the motor shaft speed as a function of time based on the behavior of the inputs can be seen in the graph in **Figure 6**.

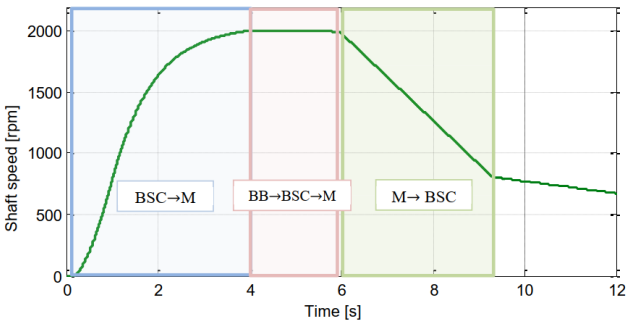

Figure 6. Evolution of ωn based on accelerator and brake signals.

It is observed that there is acceleration even after the interruption of the voltage increase in the motor terminals, where the speed reaches the steady state in 4s, a period necessary for it to overcome the inertia of the mechanical load connected to the shaft. At the instant of braking, the speed decreases linearly, because the electromagnetic and mechanical resistant torques are constant. The most interesting point occurs at t = 9.30s with the interruption of regeneration even with the persistence of brake actuation, because at this moment D4 reaches 0.8. Figure 123 shows the status signals Fr, and a>0, referring to the occurrence of regenerative braking and the angular acceleration of the motor shaft, respectively.

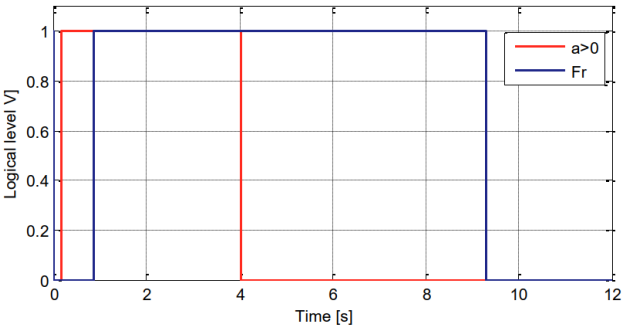

Figure 7. Status signals for acceleration and regenerative braking.

The signals shown in **Figure 7** clearly distinguish between the acceleration and braking stages. Thus, it is verified that the first occurs up to approximately 4.04s; that is, only from this point should the battery bank send energy to the supercapacitors in order to maintain its voltage. The second step remains active at the instants of time in which the cyclic ratio D4, whose behavior **Figure 8** assumes values less than or equal to 0.8.

At the beginning of the simulation, D4 equals the unit, because cn = 0, reducing as acceleration occurs. The Fr signal shown in **Figure 7** reaches a high logical level whenever D4 ≤ 0.8, and this situation indicates that braking is possible and can be initiated at any time. For the conditions adopted, its qualification occurs in 0.88s.

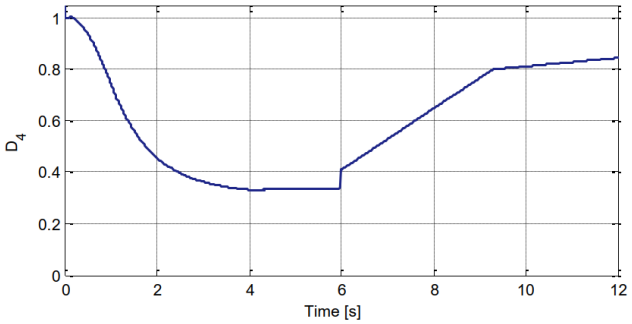

Figure 8. Temporal evolution of D4(t).

The graph in **Figure 9** depicts the behavior of the current in the armature. It is observed that during the variation of the accelerator signal the current increases, because the voltage at the terminals of the machine is increasing, and from t = 1s it decreases exponentially, becoming constant in the vicinity of t = 4s corresponds to the direction of the reinforcement current, which is positive during traction (Te > 0) and negative during regeneration (Te < 0).

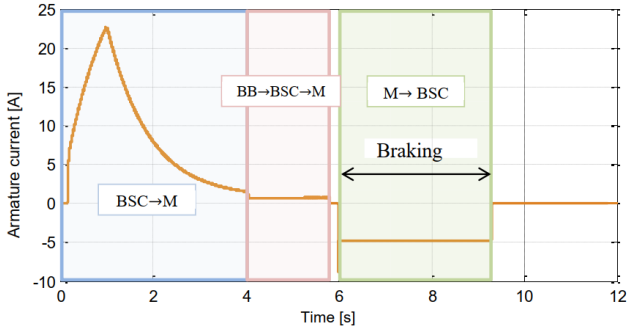

Figure 9. Armature chain in the acceleration and braking stages

When accelerating, all the energy absorbed from the DC motor originates from the supercapacitor bank. Thus, the batteries are used only when the angular velocity cn becomes approximately constant, a situation satisfied when the signal a > 0 is at a low level and Ia > 0. The graph in **Figure 10** shows this fact.

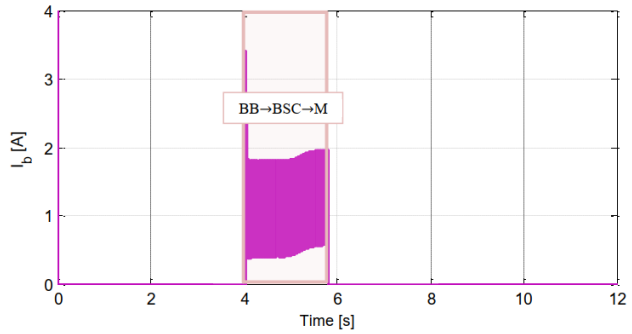

Figure 10. Battery discharge current

As can be seen, the current drained from the battery has a low magnitude since the motor operates with a load of only 0.5N.m, in addition to being zero during acceleration and after the power supply interruption to the armature at t = 5.8s. The energy generated during regenerative braking will be preferentially stored in the supercapacitor bank, thus causing an increase in its voltage, whose behavior is given by **Figure 11**. A considerable drop in Vbsc was observed between t = 0 and t = 1s due to the high current absorbed by the armature during this period. The voltages at the beginning and end of braking, equal to 232.68 and 234.72V, respectively, translate to the total amount of energy regenerated, which is equivalent to 1.20kJ.

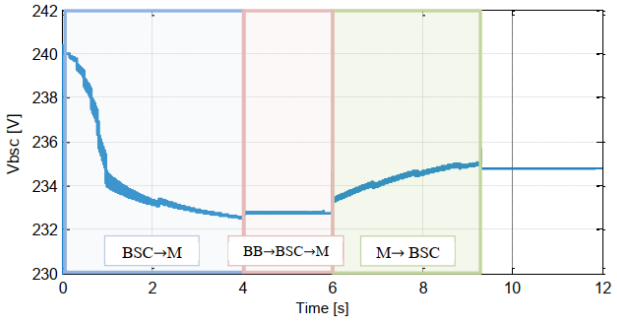

Figure 11. Voltage in the supercapacitor bank as a function of time

In order to illustrate the charging stage of the supercapacitors, the simulation will now be started with Vbsc = 185V, keeping the throttle and brake disabled. Right at the beginning, the control system notices that Vbsc is less than 190V, then initiates the discharge of the batteries at 1C (Ib = 15.60A), represented in **Figure 12**. At the end of the process, it was noted that the supercapacitors were not charged to the specified maximum voltage (210V). The reason for this is due to the influence of the Rsc series resistor, where the voltage on it is added to the Vsc during current injection. However, this is not a problem and can be compensated by increasing the indicative end-of-load value. **Figure 13** shows the temporal evolution of Vbsc in this period. In order to compare the simulated results with the theoretical ones in terms of performance, Table 18 was elaborated, where the values of mechanical energy, regenerated energy and yield are obtained via Simulink® and respectively by equations (93), (101) and (102).

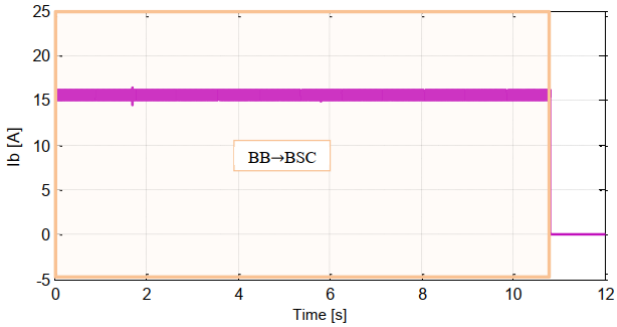

Figure 12. Discharge current of the batteries during the charge of the supercapacitors

Each of these values comes from regenerative braking processes carried out with currents from 1A to 6A, and also considers the non-idealities of semiconductors, which change depending on the current processed. In addition,

the Initial conditions are the same as those initially adopted, i.e., Vbsc = 233V, Tm = 0.5N.m.

As can be seen, the values from the simulation are very close to those calculated by the equations, where the average error concerning the yield was 4.11%. An interesting fact arises: the regenerated energy increases as more current is absorbed from the armature, but the maximum occurs at Ia = 3A for both cases. The performance follows the same behavior in the simulated system, but in the theoretical system, it remains maximum in a region delimited by currents between 3A and 4A. For better visualization, the graph in **Figure 14** was assembled.

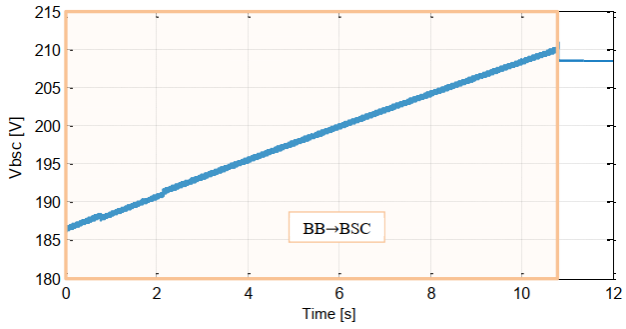

Figure 13. Bank of supercapacitors in the process of charging

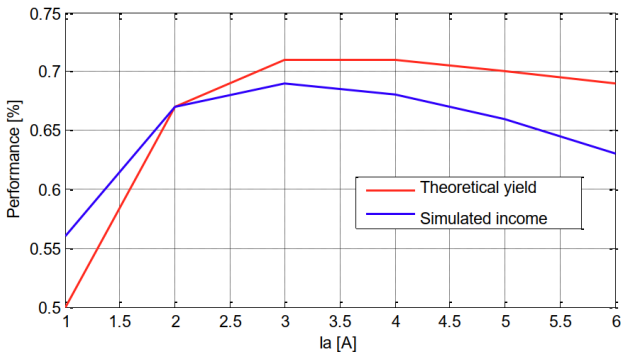

Figure 14. Comparison between theoretical and simulated yields

The regenerated energy and the yield resulting from the simulation are lower than the respective theoretical ones. The probable reason for this difference is related to the simulation itself, where the circuits of the bidirectional power converters and the DC motor, inserted in the PSIM® software, are imported by Simulink®. The signs indicated in **Figure 14** show the probable source of this difference.

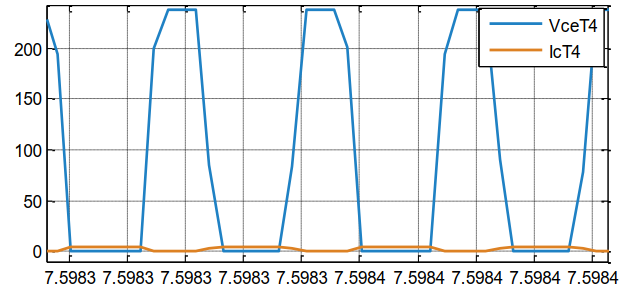

Figure 15. Voltage (VceT4) and current (IcT4) waveforms on the T4 transistor

Figure 15 represents a small interval taken from the period in which regenerative braking occurs, where the voltage and current behaviors in the T4 transistor are found during the conduction, locking, and switching phases.

In the conduction phase, the collector current is equal to that of the armature, and the voltage between the collector and emitter terminals migrates to saturation, i.e., at this moment the only source of losses is the product between the two quantities. In the blocking phase, the collector current cancels out and the transistor supports the voltage of the supercapacitor bank, a situation where losses can be disregarded. Finally, there is the crossover between Vbsc and Ia in the switching phase, as the transistor takes some time to start and stop conduction. Such crossover causes the switching losses already mentioned in the study, and they are probably responsible for the small divergence of the data presented in Table 18, since it is not possible to configure the parameters of the transistors that are part of the converter circuit regarding the switching times. Thus, the software treats them according to some method, and this does not match the behavior considered in the theoretical calculations

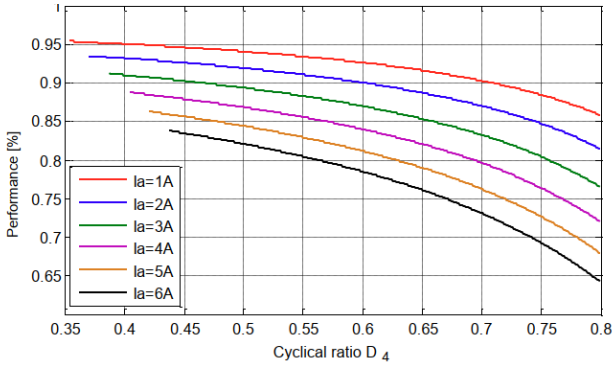

Figure 16. Yield of bi-directional converter 2 during braking for various Ia values.

Still referring to performance, it is also interesting to see how the bidirectional converter 2 behaves during regenerative braking. To discover its peculiarities, it is enough to express this magnitude in a graph as a function of the variation of D4 for various currents absorbed from the reinforcement, as shown in the graph in **Figure 16**.

It is observed that the yield decreases as the cycle ratio increases, a behavior that is characteristic of the converter Boost. In addition, it is also reduced as greater braking capacity is required, i.e., higher Ai values, as the power dissipation in the armor's resistance increases with its increase. Another point that deserves to be highlighted in the graph in **Figure 16** corresponds to the different values of the initial cyclic ratios for each absorbed current. The explanation for this phenomenon comes from the investigation of the terminal voltage of the DC motor, which represents the power supply to the converter Boost. The terminal voltage is obtained by the difference between the counterelectromotive force Ea and the product RaIa, i.e., the greater the current drained from the armor, the lower it will be Vt, thus implying the increase of D4

In steady-state cruising conditions, the batteries supplied the continuous current required to overcome motor and load losses. The voltage and current profiles showed good stability in this operating mode. The passive balancing circuits effectively avoided individual cell over-voltage during the tests.

The motor load was stepped up for the regenerative braking tests to initiate deceleration. The resulting decrease in speed caused the motor to operate as a generator, transferring power back to the supercapacitors. Recovered energy on the capacitors reached over 1200J, with system efficiency up to 65%. This demonstrates the ability to capture a significant portion of the vehicle's kinetic energy during braking.

The prototype exhibited some discrepancies between the simulated and experimental results, primarily lower efficiency during regeneration. Sources of losses include inaccuracies in model parameters, unmodeled dynamics like converter switching losses, and limitations of the digital control platform. The relatively high series resistance of the battery bank also restricted the operating current range.

However, the key functionality of the hybrid storage system and bidirectional converters was successfully validated. The supercapacitors handled current transients while the batteries provided steady power. The dSPACE controller effectively coordinated the switching of the converters in response to operating conditions and commanded current references. The results illustrate the viability of this architecture to overcome issues like limited range and battery stress in electric vehicles.

In conclusion, the prototype implemented and demonstrated the core concepts of hybrid energy storage and bidirectional power flow for electric vehicle applications. The modular design allows flexibility in the battery and supercapacitor banks to meet different voltage and energy capacity requirements. Further refinement of the system parameters and controls may improve efficiency and dynamic response. With improved range and battery longevity, adoption of electric vehicles could be accelerated by utilizing architectures based on this work.

5. Conclusions

This work presented the design, implementation, and experimental evaluation of a hybrid energy storage system for electric vehicles using supercapacitors and batteries. Bidirectional DC-DC converters were developed to actively control power flow between the energy sources and the traction motor. Regenerative braking capabilities were incorporated to recover kinetic energy during deceleration for efficiency improvements.

The use of supercapacitors as a complementary storage element to batteries helps overcome critical limitations of electric vehicles. The supercapacitors can supply high transient currents during acceleration, avoiding battery overload. They also accept charge efficiently during braking, unlike batteries, which can be damaged by sudden charging. This hybrid architecture allows the batteries to operate in an optimal steady power range.

Simulation models were created in MATLAB/Simulink to facilitate system design and testing. The control logic was deployed on a dSPACE real-time controller for hardware-in-the-loop experimentation. Custom circuit boards implemented the converters, gate drivers, sensors, and auxiliary systems. The laboratory test bench provided a flexible platform for evaluating the prototype.

Experimental results successfully validated the core functionality, including the coordination of converter switching to manage power flow. The supercapacitors supplied momentary acceleration loads over 8A, while the batteries were provided under 2A. Regenerative braking recovered over 1200J, with system efficiency up to 65%, reasonably matching predictions. This demonstrated the viability of the hybrid supply and bidirectional converters.

Opportunities for improvement remain, including mitigating the lower efficiency compared to simulations. Advanced controls may also expand the operational range. With further refinement, this architecture can help overcome barriers to electric vehicle adoption such as limited range and battery life. The prototyping approach presented enables rapid design iteration and flexibility. Overall this work validated the benefits of hybrid energy storage with reversible converters for sustainable and efficient transportation.

6. Nomenclature

SOC	State of Charge
HESS	Hybrid Energy Storage System
SC	Supercapacitor
BMS	Battery Management System
PI Controller	Proportional-Integral Controller
PWM	Pulse Width Modulation
DC-DC Converter	Bidirectional converter for managing energy flow
Regen Braking	Regenerative braking (braking that converts kinetic to electrical energy)
η_{regen}	Regenerative braking efficiency

References

Abdelghany, M. B., Shehzad, M. F., Mariani, V., Liuzza, D. and Glielmo, L. (2022). Two-stage model predictive control for a hydrogen-based storage system paired to a wind farm towards green hydrogen production for fuel cell electric vehicles. *International Journal of Hydrogen Energy*, **47**(75), 32202–32222. https://doi.org/10.1016/J.IJHYDENE.2022.07.136

Beatrice, C., Capasso, C., Doulgeris, S., Samaras, Z. and Veneri, O. (2024). Hybrid storage system management for hybrid electric vehicles under real operating conditions. *Applied Energy*, **354**. https://doi.org/10.1016/J.APENERGY.2023.122170

Charoen-amornkitt, P., Nantasaksiri, K., Ruangjirakit, K. and Laoonual, Y. (2023). Energy consumption and carbon emission assessment of battery swapping systems for electric motorcycle. *Heliyon*, **9**(12). https://doi.org/10.1016/J.HELIYON.2023.E22887

Chen, Z., Liu, Y., Ye, M., Zhang, Y. and Li, G. (2021). A survey on key techniques and development perspectives of equivalent

consumption minimisation strategy for hybrid electric vehicles. *Renewable and Sustainable Energy Reviews*, **151**. https://doi.org/10.1016/J.RSER.2021.111607

Deng, K., Liu, Y., Hai, D., Peng, H., Löwenstein, L., Pischinger, S. and Hameyer, K. (2022). Deep reinforcement learning based energy management strategy of fuel cell hybrid railway vehicles considering fuel cell aging. *Energy Conversion and Management*, **251**. https://doi.org/10.1016/J.ENCONMAN.2021.115030

Deng, K., Peng, H., Dirkes, S., Gottschalk, J., Ünlübayir, C., Thul, A., Löwenstein, L., Pischinger, S. and Hameyer, K. (2021). An adaptive PMP-based model predictive energy management strategy for fuel cell hybrid railway vehicles. *ETransportation*, 7. https://doi.org/10.1016/J.ETRAN.2020.100094

Eckert, J. J., da Silva, S. F., Lourenço, M. A. de M., Corrêa, F. C., Silva, L. C. A. and Dedini, F. G. (2021). Energy management and gear shifting control for a hybridized vehicle to minimize gas emissions, energy consumption and battery aging. *Energy Conversion and Management*, **240**. https://doi.org/10.1016/J.ENCONMAN.2021.114222

Falvo, M. C., Lamedica, R., Bartoni, R. and Maranzano, G. (2011). Energy management in metro-transit systems: An innovative proposal toward an integrated and sustainable urban mobility system including plug-in electric vehicles. *Electric Power Systems Research*, **81**(12), 2127–2138. https://doi.org/10.1016/J.EPSR.2011.08.004

Frasci, E., Cervone, D., Nacci, G., Sementa, P., Arsie, I., Jannelli, E. and Maria Vaglieco, B. (2022). Comprehensive model for energetic analyses of a series hybrid-electric vehicle powered by a passive Turbulent Jet Ignition engine. *Energy Conversion and Management*, **269**. https://doi.org/10.1016/J.ENCONMAN.2022.116092

Hasan, M. K., Mahmud, M., Ahasan Habib, A. K. M., Motakabber, S. M. A. and Islam, S. (2021). Review of electric vehicle energy storage and management system: Standards, issues, and challenges. *Journal of Energy Storage*, **41**. https://doi.org/10.1016/J.EST.2021.102940

Hu, J., Lin, Y., Li, J., Hou, Z., Chu, L., Zhao, D., Zhou, Q., Jiang, J. and Zhang, Y. (2024). Performance analysis of AI-based energy management in electric vehicles: A case study on classic reinforcement learning. *Energy Conversion and Management*, 300. https://doi.org/10.1016/J.ENCONMAN.2023.117964

Icaza-Alvarez, D., Jurado, F. and Tostado-Véliz, M. (2023). Long-term planning for the integration of electric mobility with 100% renewable energy generation under various degrees of decentralization: Case study Cuenca, Ecuador. *Energy Reports*, **9**, 4816–4829. https://doi.org/10.1016/J.EGYR.2023.03.118

Jannesar Niri, A., Poelzer, G. A., Zhang, S. E., Rosenkranz, J., Pettersson, M. and Ghorbani, Y. (2024). Sustainability challenges throughout the electric vehicle battery value chain. *Renewable and Sustainable Energy Reviews*, **191**. https://doi.org/10.1016/J.RSER.2023.114176

Khammassi, E., Rehimi, F., Halawani, A. T. M. and Kalboussi, A. (2024). Energy transition policy via electric vehicles adoption in the developing world: Tunisia as a case study. *Energy Policy*, **185**. https://doi.org/10.1016/J.ENPOL.2023.113927

Li, Y., Lin, H. and Jin, J. X. (2024). Decision-making for sustainable urban transportation: A statistical exploration of innovative mobility solutions and reduced emissions. *Sustainable Cities and Society*, **102**. https://doi.org/10.1016/J.SCS.2024.105219

Liguo, X., Ahmad, M., Khan, S., Haq, Z. U. and Khattak, S. I. (2023). Evaluating the role of innovation in hybrid electric vehicle-related technologies to promote environmental sustainability in knowledge-based economies. *Technology in Society*, 74. https://doi.org/10.1016/J.TECHSOC.2023.102283

Lu, Z., Tian, H., sun, Y., Li, R. and Tian, G. (2023). Neural network energy management strategy with optimal input features for plug-in hybrid electric vehicles. *Energy*, **285**. https://doi.org/10.1016/J.ENERGY.2023.129399

Payri, F., Guardiola, C., Pla, B. and Blanco-Rodriguez, D. (2012). On a stochastic approach of the ECMS method for energy management in hybrid electric vehicles. *IFAC Proceedings* Volumes (IFAC-PapersOnline), **45**(30), 341–348. https://doi.org/10.3182/20121023-3-FR-4025.00041

Pecolt, S., Błażejewski, A., Królikowski, T. and Kamiński, P. K. K. (2023). Application for testing and optimising the performance of electric power systems in a hybrid "MELEX" vehicle. *Procedia Computer Science*, **225**, 2634–2643. https://doi.org/10.1016/J.PROCS.2023.10.255

Qureshi, K. N., Alhudhaif, A. and Jeon, G. (2021). Electric-vehicle energy management and charging scheduling system in sustainable cities and society. *Sustainable Cities and Society*, 71. https://doi.org/10.1016/J.SCS.2021.102990

Rauf, M., Kumar, L., Zulkifli, S. A. and Jamil, A. (2024). Aspects of artificial intelligence in future electric vehicle technology for sustainable environmental impact. *Environmental Challenges*, 14. https://doi.org/10.1016/J.ENVC.2024.100854

Rele, M., Patil, D. and Krishnan, U. M. (2023). Hybrid Algorithm for Large Scale in Electric Vehicle Routing and Scheduling Optimization. *Procedia Computer Science*, **230**, 503–514. https://doi.org/10.1016/J.PROCS.2023.12.106

Ritzmann, J., Lins, G. and Onder, C. (2020). Optimization method for the energy and emissions management of a hybrid electric vehicle with an exhaust aftertreatment system. *IFAC-PapersOnLine*, **53**(2), 13797–13804. https://doi.org/10.1016/J.IFACOL.2020.12.888

Sulaiman, N., Hannan, M. A., Mohamed, A., Ker, P. J., Majlan, E. H. and Wan Daud, W. R. (2018). Optimization of energy management system for fuel-cell hybrid electric vehicles: Issues and recommendations. *Applied Energy*, **228**, 2061–2079. https://doi.org/10.1016/J.APENERGY.2018.07.087

Verma, S., Mishra, S., Gaur, A., Chowdhury, S., Mohapatra, S., Dwivedi, G. and Verma, P. (2021). A comprehensive review on energy storage in hybrid electric vehicle. *Journal of Traffic and Transportation Engineering* (English Edition), **8**(5), 621–637. https://doi.org/10.1016/J.JTTE.2021.09.001